InfraMatics
The Newsletter of Subaudible Sound

NUMBER 26 SEPTEMBER 2010

## IN THIS ISSUE

Page No.

1. Ludwik Liszka
*A Search for Underground Nuclear Test Signatures in Archival Infrasound Data*

5. Alexis Le Pichon, Robin Matoza, Nicolas Brachet, Yves Cansi
*Recent Enhancements of the PMCC Infrasound Signal Detector*

# A SEARCH FOR UNDERGROUND NUCLEAR TEST SIGNATURES IN ARCHIVAL INFRASOUND DATA

*Ludwik Liszka, Swedish Institute of Space Physics, Umeå, Sweden*

## Introduction

The infrasound project with continuous recording of infrasound started in October 1972 at Kiruna Geophysical Observatory, which later became Kiruna Geophysical Institute and, finally, the Swedish Institute of Space Physics (IRF). The recording equipment evolved through different stages: from narrow band (2 Hz) film recordings (1972-82), through the computerized version of narrow band recordings (1982-94), to the present broad-band. Computerized broad-band equipment started its operation at all arrays in 1994. The infrasound recordings in Sweden are the longest continuous time series of its kind in the world.

During the 1970s and 1980s there was a prevalent opinion that underground nuclear explosions could not be detected by measurements of atmospheric infrasound. For this reason the infrasound data collected after 1972 at Swedish infrasound arrays were never searched for signals from underground nuclear tests (UNT). Recently it has been shown by several researchers that both earthquakes and underground nuclear explosions generate infrasound in the atmosphere (e. g. Mutschlecner and Whitaker, 2005, and Whitaker, 2008). A brief search in the computerized data from the 1980s has shown that a number of underground explosions at Novaya Zemlya could be easily identified.

# Two Hz Infrasound Recordings in Northern Sweden

## A. FILM RECORDINGS

The measuring equipment developed in Kiruna used a narrow-band (6% bandwidth), fixed frequency (2 Hz), phase-detection technique which makes it possible to detect weak infrasound from point sources, far below background level. Details of the equipment have been given earlier. The main part of the equipment is a tripartite array with microphones located at (x1, y1), (x2, y2) and (x3, y3), where distances between microphones are shorter than one wavelength. Phase differences between microphone pairs 1-2 and 1-3 ($\Delta_{12}$ and $\Delta_{13}$) are measured by means of a two-channel phase comparator. These two phase differences give complete information about the wave vector of the incident wave. The wave vector may be described by the azimuth of the direction of arrival of the wave, A, and the apparent horizontal velocity of the wave across the array $V_p$. These two quantities may be calculated from phase differences $\Delta\phi_{12}$ and $\Delta\phi_{13}$, i.e.,

$$A = -\arctan\left[\frac{y_1 - y_2 - P.(y_1 - y_3)}{x_1 - x_2 - P.(x_1 - x_3)}\right] ,$$

where

$$P = \Delta\phi_{12}/\Delta\phi_{13}$$

and

$$V_p = \frac{2\pi f}{\Delta\phi_{12}} \left[(y_1 - y_2)\cos A - (x_1 - x_2)\sin A\right] .$$

Here f is the wave frequency. The above expressions have been derived by Cowling, Webb, and Yeh (1971) in their study of acoustic gravity waves. In the present work another method of presentation of the wave vector is used. A unit vector in the direction of the wave vector is projected onto the horizontal plane. Components of the projected vector X, Y describe the unit vector, since

$$Z = (1 - X^2 - Y^2)^{½}.$$

The azimuth A of the direction of arrival of the wave is then

$$A = \arctan(X/ Y),$$

and the horizontal trace velocity across the array is

$$V_p = \frac{L}{X^2 + Y^2}$$

where L is a constant which depends on the distance between microphones and on the wave frequency. The slope of the vector E may be calculated if the local sound velocity c is known:

$$E = \cos^{-1}(c/ V_p).$$

Digital equipment which converts phase differences $\Delta\phi_{12}$ and $\Delta\phi_{13}$ into components of the unit vector X, Y has been constructed.

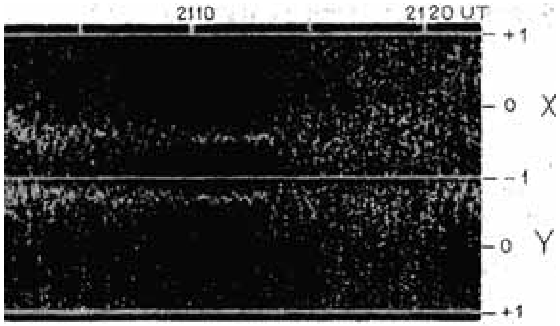

*Fig. 1. A continuous film recording of the unit vector components X and Y. One pair X, Y is obtained during each wave cycle.*

The components X and Y of the unit vector were recorded separately on a continuously moving photographic 35 mm film. An example of such a recording is shown in Fig. 1. Each simultaneous pair of coordinates X and Y gives the direction of the wave vector.

This recording method was used for routine recordings at all stations.

The azimuth of the direction of arrival of the infrasonic wave may, in many cases, be determined with an accuracy of Fig. 1. A continuous film recording of the unit vector components X and Y. One pair X, Y is obtained during each wave cycle. ≈ 1 $0^0$. Measurements of the direction of arrival at two or more stations may be used for location of infrasound sources. The accuracy of the location depends upon the distance between the stations and upon the direction to the source with respect to the line joining both stations. The accuracy of the location is increased when more than two stations are used.

The detection threshold of the equipment is, under favorable meteorological conditions, 77 dB below 1 µbar. The detection threshold may be lowered if microphones are placed in Helmholtz resonators tuned to the detected frequency.

## B. COMPUTERIZED RECORDINGS

In December 1981 all stations were computerized using a small Swedish-manufactured computer: the ABC80. The computer, in its basic model, was only equipped with RAM and a floppy disk reader for software input and storage and an audio cassette unit for the data storage. Due to the limited storage capacity, complete X, Y data could not be stored. The X, Y data were converted into the azimuth-of-arrival and the horizontal trace velocity and stored in RAM for each 30-second period, after which distributions of both variables were created. The distributions were then stored on the audio cassette at the end of each half-hour period. An example of 60 minutes of angle-of-arrival distributions during a 60-minute period is shown in Fig. 2. One audio cassette was enough to store data from approximately 10 days. Infrasound recordings based on the ABC80 were continued until May 1996. The stored data were used to construct distributions of angle-of-arrival, one distribution for each 30-second period.

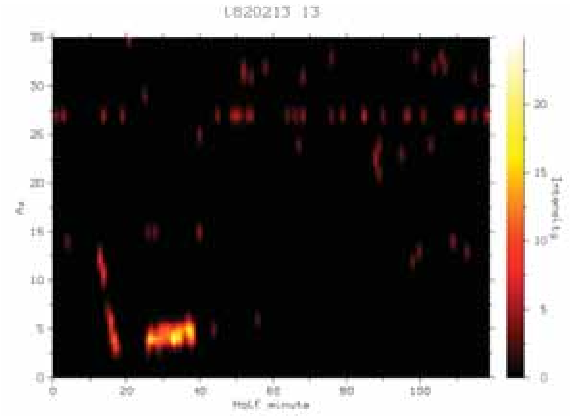

*Fig. 2. 3D distributions of angle-of-arrival from Lycksele on February 13, 1982, between 1300 and 1400 UT showing two infrasonic sources: one moving between 140 and 30 degrees and one stationary at approximately 40 degrees. Vertical scale is in 10-degree units.*

Angle-of-arrival distributions of 2 Hz signals for the entire period December 1981-May 1996 may be accessed at the IRF-Umeå home page (www.umea.irf.se/il2hz).

## A search for UNT signatures

It was assumed that underground nuclear tests performed at distances up to 2000 km, such as those at the Novaya Zemlya test site, should be detected at IRF's infrasound arrays. The information about tests was obtained from the Database of nuclear tests (www.johnstonsarchive.net/nuclear/tests). The search was limited to tests carried out during 1987-1988 at Novaya Zemlya, Northern Site (Matochkin Shar), NZ-NS. Directions to the test site and distances from all three infrasound arrays are shown in Table 1.

| Array | Direction (deg) | Distance (km) |
|---|---|---|
| Kiruna | 48.8 | 1382 |
| Jämtön | 41.9 | 1473 |
| Lycksele | 40.0 | 1693 |

*Table 1. Directions and distances to the NZ-NS test site*

There were three tests during the investigated period, all with a total yield of 150 kt:

1987-08-02 at 02:00:00 UTC, geographical coordinates 73.326 N 54.602 E.

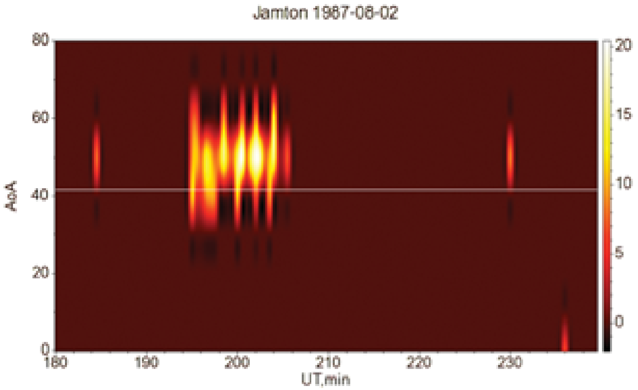

*Fig. 3. The azimuth distribution of infrasound signal from the UNT of 1987-08-02 recorded at the Jämtön array. X-axis in minutes UT. The white horizontal line indicates the great circle direction to the test site.*

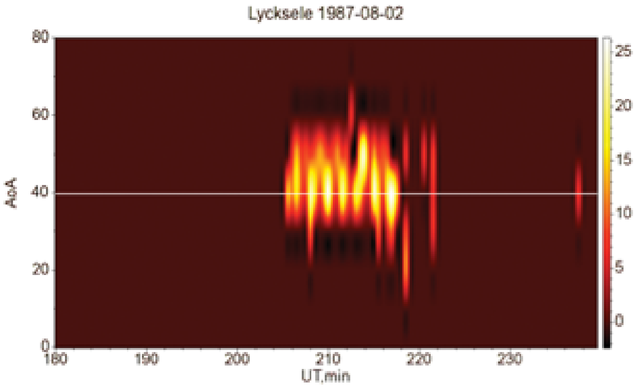

*Fig. 4. The azimuth distribution of infrasound signal from the UNT of 1987-08-02 recorded at the Lycksele array. X-axis in minutes UT. The white horizontal line indicates the great circle direction to the test site.*

The modulation visible on both distributions is most likely a propagation effect.

1988-05-07 at 22:49:58 UTC, geographical coordinates 73.314 N 54.553 E.

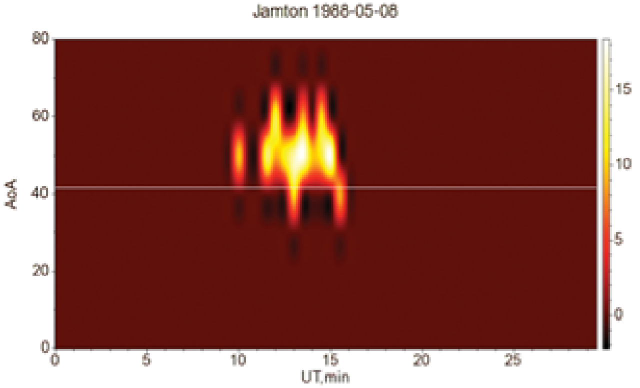

*Fig. 5 The azimuth distribution of infrasound signal from the UNT of 1988-05-07 recorded at the Jämtön array. X-axis in minutes UT. The white horizontal line indicates the great circle direction to the test site.*

1988-12-04 at 05:19:53 UTC, geographical coordinates 73.366 N 55.001 E.

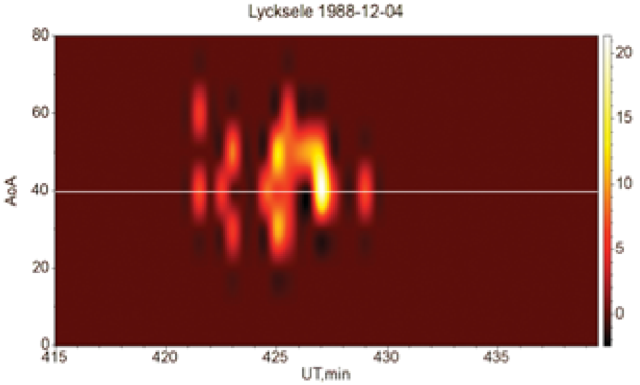

*Fig. 6 The azimuth distribution of infrasound signal from the UNT of 1988-12-04 recorded at the Lycksele array. X-axis in minutes UT. The white horizontal line indicates the great circle direction to the test site.*

The infrasound data stored in the data base contains only one-hour intervals during which significant signals were detected. It is, therefore, not possible to know, using the 2 Hz data base, if signals from the UNT were completely absent at other arrays. For example, none of the three tests can be found in the Kiruna data. The reason may be that the computer software at that time was not very sophisticated and decided that there were no significant signals and therefore the hour was not saved. Another reason to skip the particular hour could be equipment malfunction. Only the original film recordings could give the complete information about the occurrence of particular signals. That would require scanning the entire collection of films.

## Conclusions

The present brief study of archival infrasound data from arrays in Northern Sweden shows that medium-size underground nuclear tests are, in fact, visible in 2 Hz narrow band recordings at distances of the order of 2,000 km. A careful study of the entire period 1973-1994 could therefore provide valuable data on infrasound generation by the UNTs. In particular, the data collected during the 1970s, when large UNTs also took place, could be of considerable interest.

The film- and computerized recordings, collected during those 21 years, contain values of components of the 2Hz wave vector. There is, consequently, no direct information about the signal's amplitude. During the 1990s, there was a period when the 2 Hz recordings and the computerized broad-band recordings were run in parallel. That period may be used for the purpose of calibration and a measure of the signal-to-noise ratio may be derived from the film recordings.

## References

Cowling D. H., Webb H. D. and Yeh K. C.: 1970 Tech. Rep. 38, Ionosph. Radio Lab., Univ. of Illinois.

Mutschlecner J. P. and R. W. Whitaker: Infrasound from earthquakes. JGR Vol. 110, 1108, 2005.

Whitaker R. W.: Infrasound signals from ground-motion sources. In: *2008 Monitoring Research Review: Ground-Based Nuclear Explosions Monitoring Technologies,* 2008.

## Contact the Author

Ludwik Liszka Swedish Institute of Space Physics, SE-901 87 Umeå, Sweden, e-mail:ludwik.liszka@irf.se, phone +46 90 7869205.

# RECENT ENHANCEMENTS OF THE PMCC INFRASOUND SIGNAL DETECTOR

*Alexis Le Pichon, Robin Matoza, Nicolas Brachet, Yves Cansi*
*CEA/DAM/DIF, F-91297 Arpajon, France*

## Context

The Progressive Multi-Channel Correlation Method (PMCC), originally designed for seismic arrays, proved efficient at detecting low-amplitude, coherent infrasonic signals within incoherent noise (Cansi, 1995; Cansi and Klinger, 1997; Le Pichon and Cansi, 2003).

The PMCC detector was originally developed by the CEA/DASE and was installed in 2004 in the operational environment of the International Data Centre (IDC) of the Comprehensive nuclear Test-Ban Treaty Organization (CTBTO) in Vienna, Austria. PMCC has performed well in terms of detection sensitivity and robustness.

Atmospheric infrasound signals are observed across a wide frequency range (~0.01-20 Hz, Campus and Christie, 2010). We may consider three general frequency bands of interest:

- Above 0.5 Hz: impulse signals of natural or man-made origin, which may propagate over distances of several hundred kilometers.
- Between 0.1 and 0.5 Hz: microbaroms and isolated large remote events such as explosions, meteorites and volcanoes.
- Below 0.1 Hz: large-scale atmospheric disturbances such as mountain associated waves and auroral infrasound.

For each of these frequency bands, PMCC parameters must be optimized at a compromise between a low detection level and a low number of false alarms. One of the major differences between these configurations is the duration of the sliding time-window and the frequency band spacing.

For standard processing of IMS-type infrasound arrays, the window length required ranges from tens to hundreds of seconds. In previous releases of WinPMCC, the window length remained constant during a processing run. Hence, previous PMCC processing at the CEA/DASE was performed in multiple separate, independent runs with different target signal frequencies.

During the last 5 years, several changes have been made to enhance the PMCC source code at the CEA/DASE (WinPMCC) and at the IDC (DFX/Geotool-PMCC). Studies have shown the benefit of implementing an adaptive window length and log-spaced frequency bands (Brachet et al., 2010).

## Frequency-dependent parameters

Figure 1 illustrates the window lengths and frequency bands considered in two separate standard PMCC processing runs used to target low- (0.02-0.5 Hz) and high-frequency (0.1-4 Hz) bands. This is compared to a new single processing run with log-spaced frequency bands (0.01-5 Hz) and window lengths that vary linearly with the period.

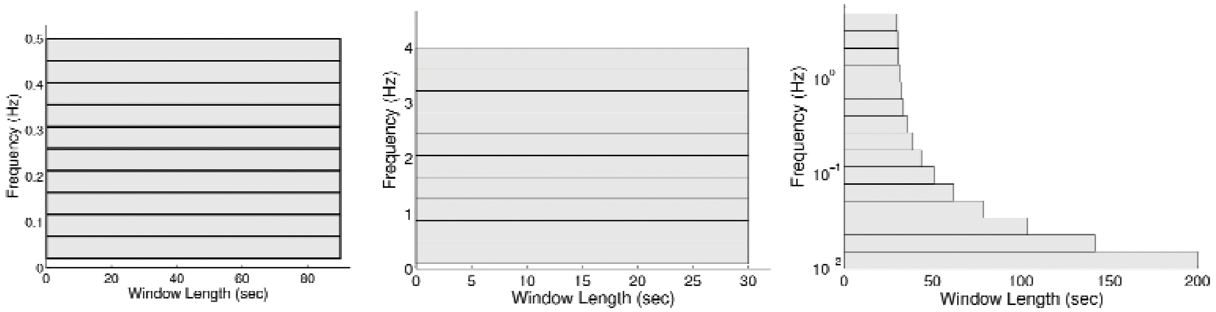

*Fig 1. Examples of two 10-band standard configurations for low- and high-frequency processing (0.02-0.5 Hz and 0.1-4 Hz, left and middle respectively), replaced by a single configuration consisting of 15 bands with log-spaced filter parameters (0.01-5 Hz) and a variable window length.*

In addition to the window length, bandwidth and filter parameters (filter order and ripple), the following detection parameters can now be adjusted as a function of frequency:

- TimeStep (s): overlap between two consecutive time windows is now defined as a fraction (%) of the window length.
- ThresholdNbSensors: minimum number of sensors required for detection.
- QLambda: threshold distance Q.λ for integration of a new sensor in a growing sub-network (aggregation of a new sensor if its distance from the barycentre of the growing sub-network is smaller than Q.λ).
- ThresholdConsistency (s): maximum consistency and threshold for detection.

Also, the parameters controlling the clustering of detections (pixels) into families can be varied as a function of frequency:

- ThresholdDate (s): maximum time difference between a pixel and a family.
- ThresholdDistance: maximum acceptable dimensionless Euclidean distance in the time-frequency-speed-azimuth domain when integrating a candidate pixel into a growing family.
- Sigma_t (s): maximum distance in time between a given pixel and a family. It must be higher than TimeStep, otherwise no integration of pixel in family can occur. If no more pixels can be integrated because of this condition, the family is closed.
- Sigma_f (Hz): maximum distance in frequency for integration of a pixel into a family.
- Sigma_a (°): maximum distance in azimuth for integration of a pixel into a family.
- Sigma_v (%): maximum distance in velocity for integration of a pixel into a family.

For full explanations of these parameters, the reader is referred to the WinPMCC User Manual.

## Application to IMS data

Figure 2 presents an example of multi-year processing using a single log-spaced configuration (Figure 1) at IMS station IS22 (New Caledonia). Two main natural sources of infrasound waves are detected:

- Below 0.1 Hz, signals consistent with Mountain Associated Waves (MAW) generated by tropospheric wind flow over high mountain ranges are detected.
- From 0.1 to 0.4 Hz, microbaroms are continuously observed. In the southern hemisphere, microbarom signals (e.g., Garcés et al., 2004) are mainly produced by large swell systems and severe storms driven by strong continuous eastward surface winds, circulating along the Antarctic Circumpolar Current (ACC). When monitored over several years, a clear seasonal transition in the bearings along with the stratospheric general circulation between summer and winter is observed.
- Above 0.5 Hz, at backazimuths between 0-50°, persistent detections are associated with active volcanoes in the Vanuatu archipelago (Lopevi/Ambrym, and Yasur). As with microbaroms, seasonal azimuthal variations are observed. These volcanic signals arrive with unique backazimuth values and dominant frequencies resulting from differences in propagation (Le Pichon et al., 2005).

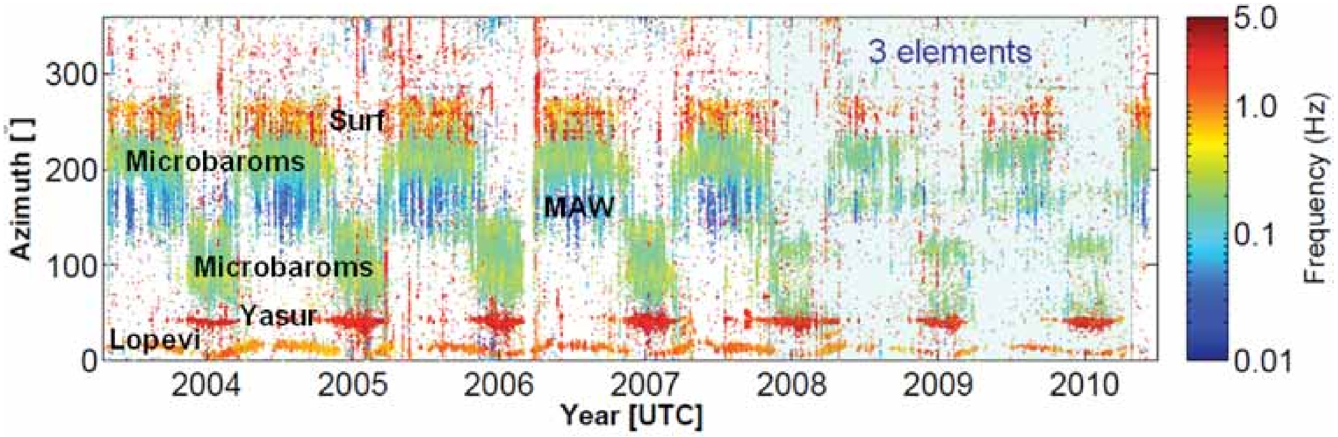

*Fig. 2. PMCC processing of IS22 (New Caledonia) from 2003 to 2010 using the 15-band log-scaled filter parameters (0.01-5 Hz) and variable window length illustrated in Figure 1. From 2008 to 2010, the reduced detection capability is explained by a missing central array element.*

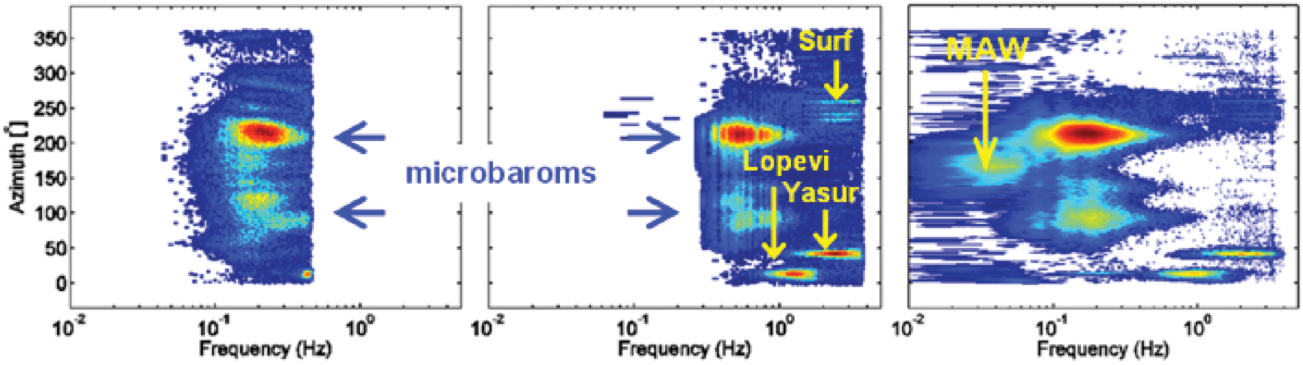

*Fig. 3. Comparisons between processing results using two 10-band low- (0.02-0.5 Hz) and high-frequency (0.1-4 Hz) configurations (left and middle, respectively) and a 15-band log-spaced configuration (0.01-5 Hz, right). Warm colors correspond to increasing number of detections in frequency-azimuth space.*

- Above 1 Hz, in the backazimuth range from 230–260°, signals are caused by surf action (e.g., Arrowsmith and Hedlin, 2005). Ocean waves from low-pressure systems in the south Pacific propagating towards New-Caledonia generate such signals when breaking on its reefs.

Figure 3 compares processing results from the standard low- and high-frequency configurations and the new log-spaced configuration (Figure 1) applied to IS22 2004-2006. The main results are:

- The main sources detected independently using the low- and high-frequency configurations are also clearly detected using the log-spaced processing (e.g., microbaroms, volcanoes and surf signals).
- With the high-frequency configuration, coherent microbarom signals are found up to 1 Hz, whereas in the log-spaced processing they are found between ~0.1-0.4 Hz. The log-spaced processing allows a more accurate estimation of signal frequency content, particularly at low frequencies.
- Between 20 and 50 s periods (0.02-0.05 Hz), during the austral winter, signals consistent with MAW are detected using the log-spaced processing. The corresponding backazimuths range from 180-200°. These signals, perhaps produced over high mountain ranges in New Zealand, have also been reported at much larger range at IS55 (Windless Bight, Antarctica) (Wilson and Olson, 2003).

## Conclusion

These results clearly show that the log-frequency-spaced implementation of PMCC is well-adapted for infrasound data processing across a wide frequency range (more than two decades) in a single processing run. There are several advantages to this new process:

- Only one processing run is necessary to cover the full frequency range of interest.
- There is no need to develop grouping methods for signals appearing in separate PMCC processing runs.
- A smoother, more continuous sampling of parameter frequency space (no discontinuities).
- Improved accuracy of estimated frequency dependent wave parameters (enables better source detection and discrimination).
- Shorter computation time (~1 week to process 2 years of data for one 4-element array on one Intel® Xeon® Processor X5460 @3.16 GHz Linux system).

The new release of the WinPMCC and PMCC detection algorithm software, running under Windows or Linux operating sytems, allows full configuration of filtering and detection parameters as described in this article and is now available by request.

## References

Arrowsmith, S., and M. Hedlin (2005), Observations of infrasound from surf in southern California, *Geophys. Res. Lett.,* 32, L09810, doi:10.1029/2005GL022761.

Brachet, N., D. Brown, R. Le Bras, P. Mialle and J. Coyne (2010), Monitoring the Earth's Atmosphere with the Global IMS Infrasound Network in Infrasound Monitoring for Atmospheric Studies, ISBN: 978-1-4020-9507-8, Springer.

Campus, P., and D. Christie (2010), Worldwide observations of infrasound waves in Infrasound Monitoring for Atmospheric Studies, ISBN: 978-1-4020-9507-8, Springer.

Cansi, Y. (1995), An automatic seismic event processing for detection and location: the PMCC method, *Geophys. Res. Lett.*, 22, 1021-1024.

Cansi, Y. and Y. Klinger (1997), An automated data processing method for mini-arrays, *CSEM/EMSC European-Mediterranean Seismological Centre, NewsLetter* 11, 1021-1024.

Garcés, M., M. Willis, C. Hetzer, A. Le Pichon, and D. Drob (2004), On using ocean swells for continuous infrasonic measurement of winds and temperature in the lower, middle, and upper atmosphere, *Geophys. Res. Lett.,* 31, L19304, DOI:10.1029/2004GL020696.

Le Pichon, A. and Y. Cansi (2003), *PMCC for Infrasound Data Processing, NewsLetter 2*, http://inframatics.org.

Le Pichon, A., E. Blanc, and D. Drob (2005), Probing high-altitude winds using infrasound, *J. Geophys. Res*., 110, D20104, DOI:10.1029/2005JD006020.

Wilson, C., and J. Olson (2003), Mountain Associated Waves at 153US and 155US in Alaska and Antarctica in the Frequency Passband from 0.015 to 0.10 Hz, Inframatics (inframatics.org), Newletters no3.

## Contact the Authors

Alexis Le Pichon: alexis.le-pichon@cea.fr

Robin Matoza: robin.matoza@cea.fr

Yves Cansi: yves.cansi@cea.fr

Nicolas Brachet: nicolas.brachet@cea.fr